

Numerical Modeling of 3D Magnetic Field Topology under RMPs and the comparison with experimental observations on EAST

Manni Jia^{1,2}, Y. W. Sun², F. C. Zhong¹, L. Wang, K. Gan, & EAST teams²

¹*College of Science, Donghua University, Shanghai 201620, People's Republic of China*

²*Institute of Plasma Physics, Chinese Academy of Sciences, Hefei 230031, China*

Email: jiamanni@mail.dhu.edu.cn

ABSTRACT

A numerical code using field line tracing for modeling the three-dimensional magnetic field topology under resonant magnetic perturbations (RMPs) has been developed and applied in Experimental Advanced Superconducting Tokamak (EAST) 2014 campaign. Currently, the model is simplified by using vacuum paradigm and neglecting the toroidal field ripple.

The modeling result predicts that the possible strike point splitting on plasma facing component and the lobes like structure on the boundary are observable in various diagnostics at different locations. It is shown that the strike point splitting strongly depends on the edge stochasticity, which is a combined effect of both perturbation spectrum and equilibrium properties.

In a lower single null configuration, it is found that RMP may also change the magnetic structure near the upper x-point and form a similar strike point splitting on the upper divertor. It depends on the distance between the two separatrix, which threshold value depends on both the RMP strength and the equilibrium properties.

To examine the RMP system on EAST and its effect on plasmas, some experiments with RMPs were held in the 2014 campaign. The static and rotational perturbation were both tested and results confirm the RMP efficiency. Particle flux profiles on divertor targets measured by divertor probes had verified the existing strike point splitting induced by RMPs. The results are consistent with the numerical modeling within measurement uncertainties and confirm the edge stochasticity induced by RMPs.

Background

H-mode is a favored experimental regime on various tokamak devices and a promising operation mode of ITER and other future reactors. The accompanied repetitive instabilities, known as edge localized modes (ELMs), help to release impurities out of plasma region but on the contrary, especially the so-called Type-I ELMs, release large amounts of particles and energy flux directly to the first wall and divertor target plates, which will become a threat to the lifetime of divertors and other plasma facing components. Furthermore, impurities being sputtered from the wall may enter the core then cause energy losses and even disruptions. According to the estimation by Hawryluk[1], there will be about 0.2-20MJ energy loss per ELM eruption on ITER similar shape and collisionality, about 20 times of the suffering limit of current material candidates (carbon fiber or tungsten). So ELM-control has become a hot topic in fusion research. The goal of ELM control is to eliminate ELMs or increase the ELM frequency and reduce the extent. At the same time, fine confinement properties should be kept as far as possible. Resonant magnetic perturbations, lower hybrid waves and pellet injection etc. are all reported with ELM control ability.

As one of the effective way to control ELMs, resonant magnetic perturbations (RMPs) have been put into use in various tokamak devices. One highlight is the experiments with $n=3$ RMPs on DIII-D which have achieved reproducible elimination of Type-I ELMs during H-mode[2][3][4]. Similar experiments on JET, MAST, ASDEX-Upgrade, NSTX, KSTAR were also carried out but the ELM-control effects vary a lot among different devices and different experiment parameters. So the physical mechanism of ELM-control is still unclear. More experimental and theoretical researches should be made.

The understanding of the 3D magnetic field topology formed due to the RMPs is significant for the study of ELM-control mechanism. The separatrix and strike point splitting have been observed during RMP experiments[5][6][7]. The 3D topology as well as theoretical edge stochastic degree induced by RMPs can be modeled and calculated with numerical methods. The modeling results on MAST, JET, DIII-D etc. have played important roles in ELM-control analysis and successfully predict the topology changes induced by magnetic perturbations.

EAST is an ITER-like tokamak and it can provide important experimental experiences for ITER. And in steady long pulse operation on EAST, it is necessary to demonstrate the capability of handling the large transient heat load induced by type-I ELMs on divertor and PFCs.

RMP coils on EAST

One RMP coil system designed for ELM control, error field studies and resistive wall mode (RWM) control has been installed on EAST in 2014[8][9]. There are two in-vessel up-down symmetric arrays. Each array has 8 coils uniformly distributed along the toroidal direction, and each coil has four turns. Their location can be seen in Figure 1. With enough power supplies, the RMP-coil system is flexible in generating perturbation spectrum. The maximum coil current is designed to be 2.5 kA per turn. Besides, the perturbation spectrum can be switched during one shot as Figure 2 shows.

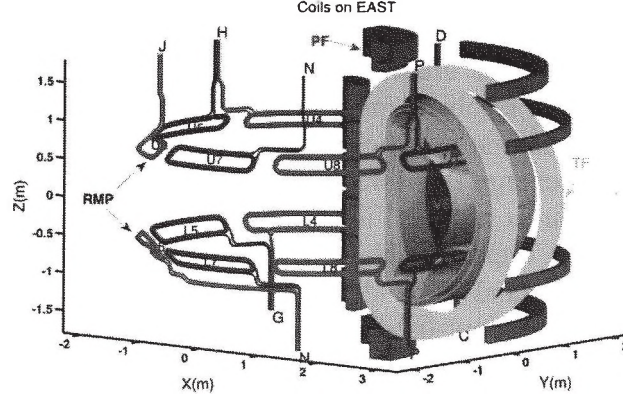


Figure 1. RMP coils on EAST

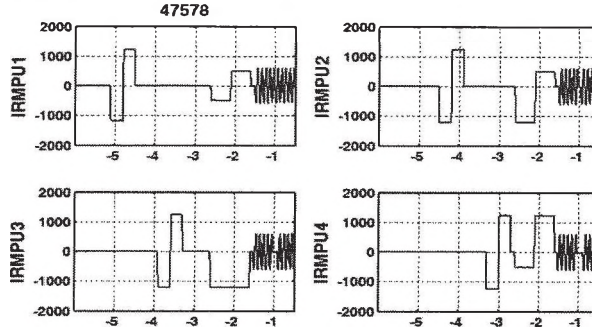


Figure 2. An example of the flexible perturbation spectrum switching of RMP coils on EAST.

Numerical Modeling of 3D magnetic topology

The basic method to model the magnetic field topology is field line tracing. We have developed MAPS code for RMP perturbation spectrum analysis [8] and there is one module named TOP2D, which is developed for modeling 3D magnetic topology both inside and outside separatrix[10]. The field line is traced by integrating two dimensional field line equations in laboratory coordinate with fixed step size $d\phi$,

$$\begin{cases} \frac{dR}{dl_\phi} = \frac{\partial}{\partial Z} \left(\frac{\psi_p}{g} \right) \\ \frac{dZ}{dl_\phi} = -\frac{\partial}{\partial R} \left(\frac{\psi_p}{g} \right) \end{cases} \quad (1)$$

where $dl_\phi = R d\phi$ and g is a function of ψ_p . Here ψ_p is the combination of equilibrium part ψ_{p0} and the perturbation $\bar{\psi}_p$. As RMP coils are separated along torus, the actual perturbation spectrum contain components with a set of mode number n . To save time, the perturbation of every (R, Z) grids can be written with subscript of mode number n as,

$$\bar{\psi}_p = \sum_n \bar{\psi}_{pn}(R, Z) e^{im(\phi + \phi_0)}. \quad (2)$$

Here ϕ_0 is the tracing initial toroidal location and $n=1,2,\dots$ can be chosen and combined freely according to the calculation demand.

Field line tracing can start at points on poloidal planes, divertor plates, or any other points of interest. The tracing of one field line will be terminated when it crosses PFCs or the tracing turn has reached the initially set maximum turns. The topology

structure can be presented with Poincaré plot and magnetic footprint patterns. Figure 3 shows the Poincaré plot of even $n=2$ RMPs. Figure 4 shows the footprint of even $n=1,3$ and 4 RMP fields.

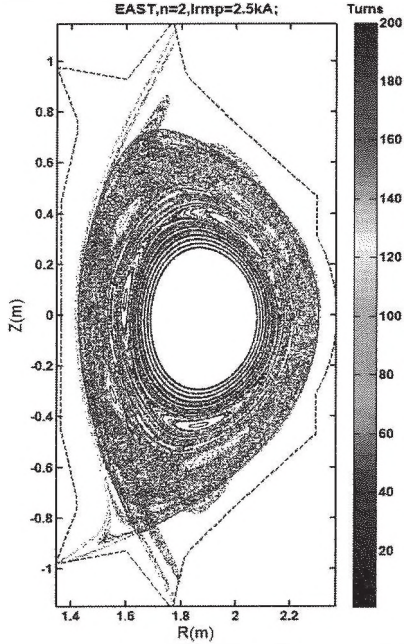


Figure 3. Poincaré plot of even $n=2$ RMPs on $\phi = 0^\circ$.

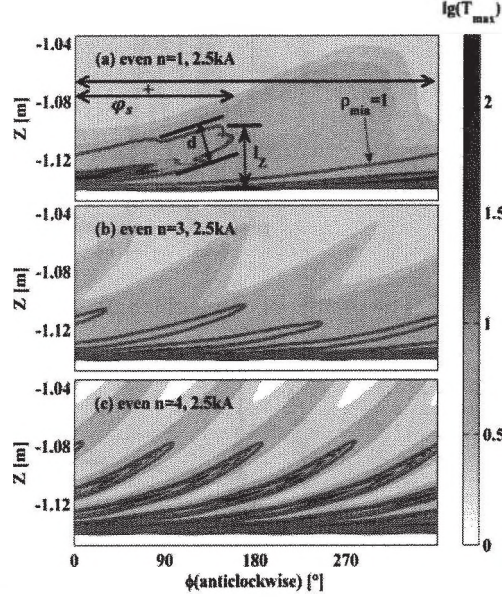


Figure 4. Footprint patterns of even $n=1,3,4$ RMPs. In (a) the three parameters to estimate the splitting degree is labeled.

Three parameters are used to characterize footprint's splitting degree. They are labeled on Figure 3(a) as we choose strike points with $\rho_{min} = 1$ as the new formed 3D separatrix. The first parameter is the width of each stripe d . The second is the splitting width in vertical direction from the peak to the bottom of the stripe represented by l_z . And the third is the total toroidal angle that each stripe covers ϕ_s .

We study the dependence of strike points splitting on edge stochasticity by TOP2D code. Edge stochasticity is measured by stochastic layer width $W_{sto} = 1 - \rho_{\sigma=1}$, where $\rho_{\sigma=1}$ represents the innermost normalized flux with Chirikov parameter $\sigma_{chr} \geq 1$. The modeling results shows that with same coil configuration, the ramp-up coil current will make wider stochastic region in the plasma boundary and make the splitting larger. The splitting degree at lower outer divertor on $\phi = 100^\circ$ of ramp-up coil current is shown in Figure 5. The edge stochasticity and the splitting degree parameters can be seen in Figure 6. We use three plasma equilibriums of different q profiles ($q_{95}=3.0, 4.5$ and 6.0 respectively.) They are obtained from equilibrium modeling based on the EAST experimental discharge of shot 38300 at 3.9s[11]. With q_{95} increasing in this case, the resonant components become stronger and the stochastic layer in the edge becomes wider, so strike point splitting is become stronger. It can be referred by the much larger connection length and wider peaks region in Figure 7.

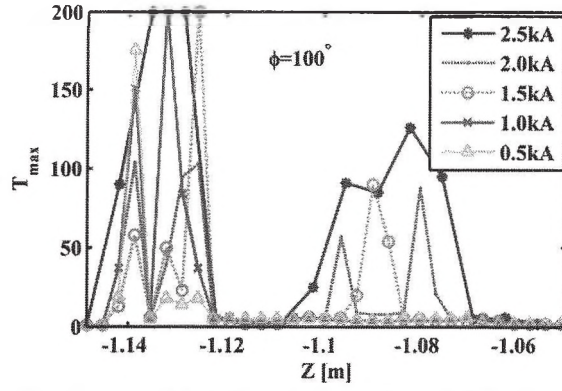


Figure 5. The profile of connect length of strike points distributed on $\phi = 100^\circ$.

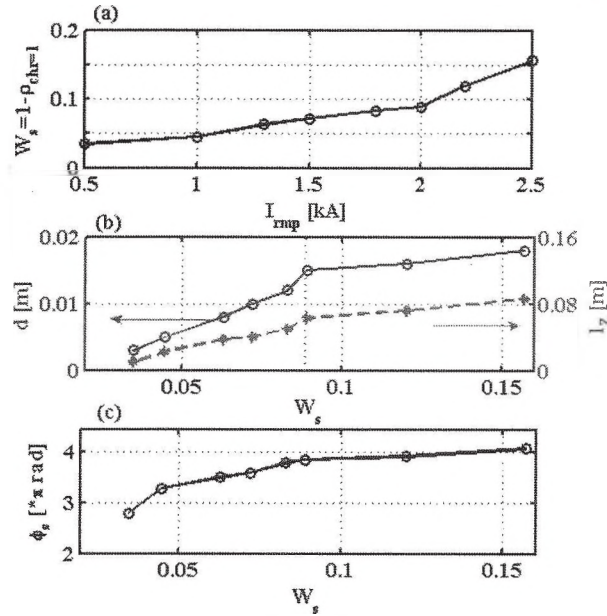


Figure 6. Footprints' characteristics for I_{RMP} scanned from 0.5 kA to 2.5 kA. The dependence of stochastic width on coil current is shown in (a). The dependence of the stripe width d and peak-bottom distances l_z on W_s are shown in (b). (c) shows the dependence of the covered toroidal angle of each stripe on W_s .

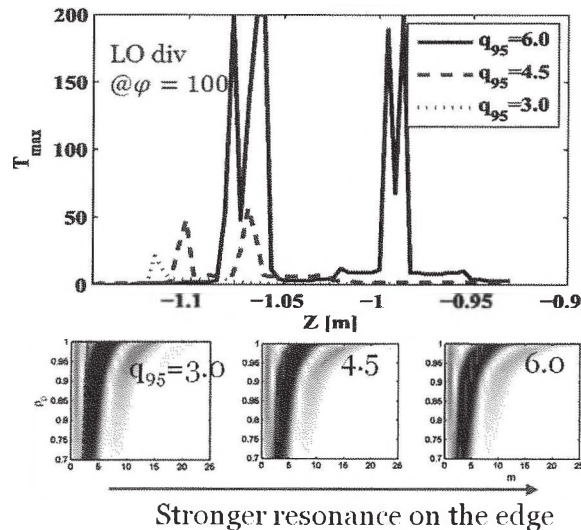


Figure 7. The connection length profiles when $q_{95}=3.0, 4.5$ and 6.0 . As the edge magnetic surface move into the stronger resonant part of the spectrum, larger splitting was caused.

We also discussed the upper strike point in near-DN configurations. dR_{sep} is defined as the physical radial separation of the X-points' flux surfaces. A similar strike point splitting appears on the upper divertor induced by RMP in a near-DN on EAST. It depends on the distance between the two separatrix. To avoid the upper strike points near the upper x-point, it is necessary to keep the distance between the two separatrix larger than a threshold value that depends on the RMP strength and the equilibrium properties.

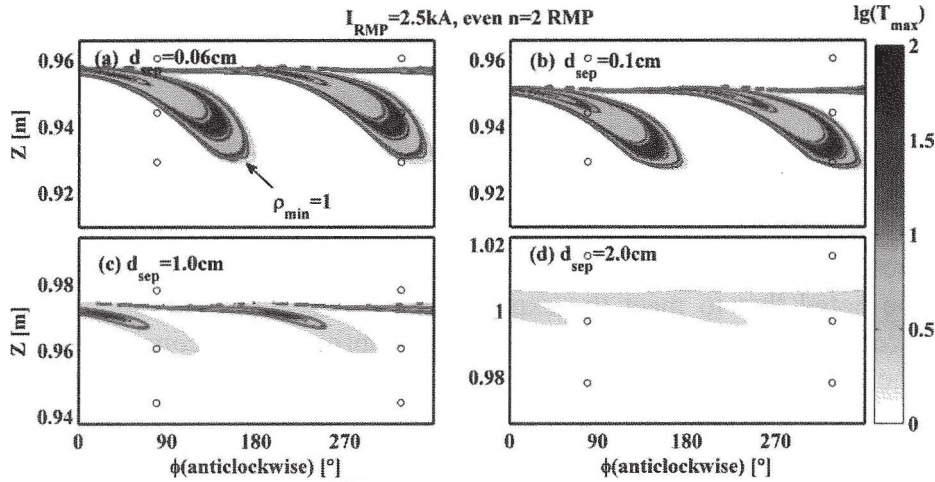


Figure 8. The footprints on UOdiv of $|dR_{sep}| = 0.06\text{cm}$ (a), 0.1 cm (b), 1.0 cm (c) and 2.0 cm (d). Points are superimposed with colors represent $\lg(T_{max})$. The red line overlaid on each subgraph is the contour line of strike points with $\rho_{min} = 1.0$. Note that the vertical axis of four subgraphs is in different Z range because the strike region is changing. But the scales are kept unchanged.

Recent experimental observations in EAST RMP experiments

RMP experiments have been primarily operated in the EAST 2014 campaign. The experimental observations are compared with the numerical modeling. Highspeed visible CCD camera, infrared CCD camera and divertor probes all observed strike point splitting during RMP experiments.

The visible and infrared high-speed CCD cameras which observe the poloidal section of vacuum vessel and part of the divertors are possible to be used for observing the lobes on the boundary and strike point splitting. The spacial resolutions are about 3mm (visible) and 4mm (infrared). One example of the observed heat load patterns on lower-outer divertor is presented in Figure 9.

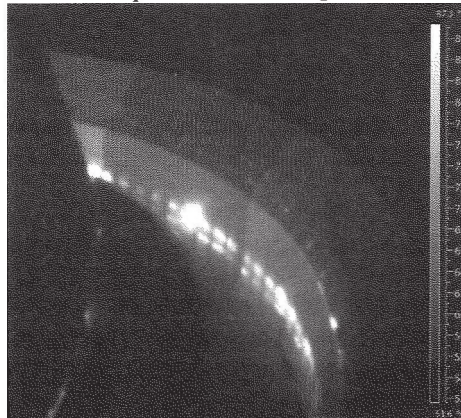


Figure 9. Heat load patterns observed by infrared CCD camera in shot 47004, which related to strike point splitting resulted by RMP fields.

The divertor probe arrays measure particle fluxes on divertor targets. The spatial resolutions of divertor probes on EAST are about 12-18mm (upper) and 10-15mm (lower). The probes on upper divertor are located at D port and O port while those on lower divertor are located from D port to O port.

In shot 52340, static even $n=1$ RMPs are applied from 3.2s to 3.5s. The coil current is 10kAt. The plasma during this time is with $B_0=2.3T$, $I_p=400kA$ and $q_{95}=5$. The signals of divertor probes are shown in Figure 10. The subfigure (a), (b) and (c) represent the time evolution of upper-outer probes in D port, O port and lower-outer probes from D to G port respectively. We compared these signals with numerical modeling result and plotted in Figure 11. We use simulated T_{max} profiles along the corresponding probe location to make comparison with saturated ion flux (j_s in A/cm^2) measured by divertor probes. The j_s profiles without and with RMP is plotted by red circles and blue dashed lines respectively. The simulated T_{max} profiles are plotted by green lines. The new formed peaks are obvious and marked by the dotted red line. It should be noted that to meet the experimental observation the simulated results is shifted accordingly as the green arrows in each subfigure. The considerable mismatch may come from errors of EFIT calculation, tracing assumptions and measuring error. It will be checked carefully in future experiments.

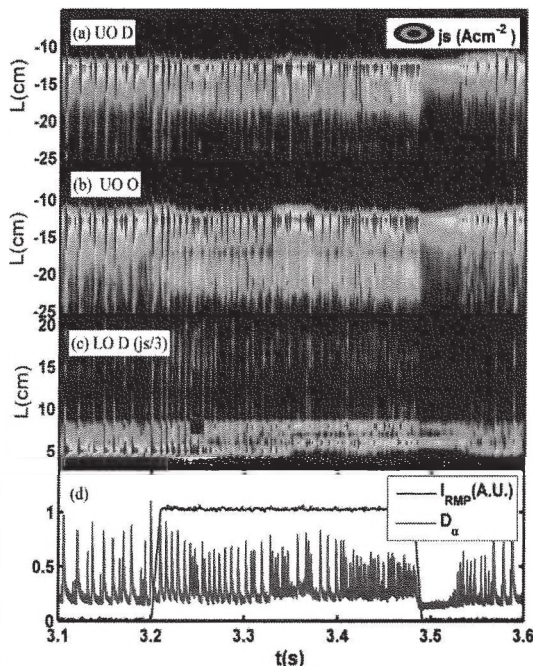


Figure 10. Profiles of saturated ion fluxes measured by divertor probes in upper-outer D port (a) and O port (b) and lower-outer D-G port (c).

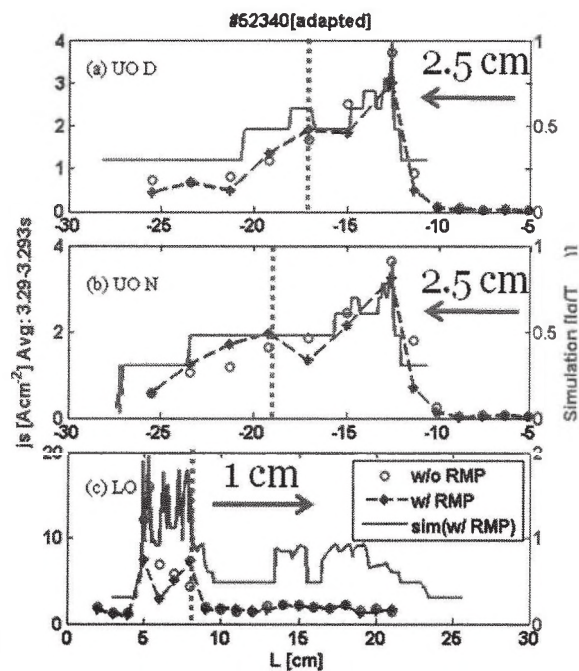


Figure 11. The experiment signals are compared with the simulated results.

In shot 52342, we tested rotate RMP fields from 3.2 to 3.5 s, as shown in Figure 12 (d). The coil current is 10kAt. The plasma parameters is almost the same with that of shot 52340. The RMP fields is even $n=1$. The j_s signals are shown in Figure 12 (a) to (c). The overlapped red contours are the simulated ρ_{min} contours without any shift. The observed structure is almost coincide with the vacuum simulated results, except a little inconformity in L direction. The structure observed by divertor signals again proved the effect of the RMP field, which will generate 3D magnetic topology.

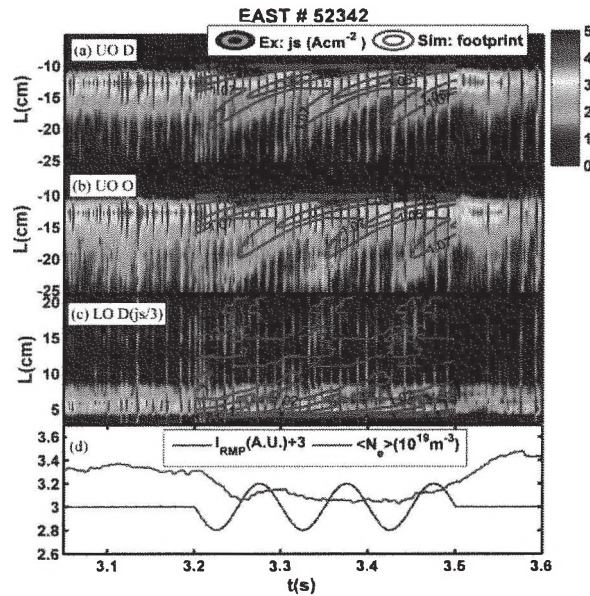


Figure 12. In shot 52342, even $n=1$ rotate RMP fields are applied in three periods from 3.2 s to 3.5s. Saturated ion fluxes profiles of upper-outer divertor probes and lower-outer divertor probes are presented and overlapped with simulated results. In general, the 3D structure presented by probe signals and the simulated results are almost consistent.

Summary

3D Magnetic topology under RMPs with lobes on the plasma boundary and strike point splitting on the divertor board is modeled by TOP2D code. The splitting degree has close relation with the edge stochasticity, which is determined both by RMP spectrum and equilibrium parameters, according to the numerical modeling.

The RMP experiments on EAST have shown the efficiency of RMPs on ELM mitigation. The divertor probes detected the splitting of particle fluxes on divertor board, and the results are almost consistent with numerical modeling results.

Plasma response and toroidal ripple will be considered in the modeling and more experiments will be done in the future. The process of stochastic transport will then be studied.

References

- [1] R. J. Hawryluk *et al.*, 2009 Nucl. Fusion **49**, 065012
- [2] T. Evans *et al.*, 2005 Nucl. Fusion **45**, 595
- [3] T. Evans *et al.*, 2004, Phys. Rev. Lett. **92**, 235003
- [4] M. E. Fenstermacher *et al.*, 2007, J. Nucl. Mater 363-365, 476
- [5] M. W. Shafer *et al.*, 2012 Nucl. Fusion **52**, 122001
- [6] D. M. Harting *et al.*, 2012 Nucl. Fusion **52**, 054009
- [7] A. Kirk *et al.*, 2012 Phys. Rev. Lett. **108**, 255003
- [8] Y. Sun *et al.*, 2014 'Modelling of non-axisymmetric magnetic perturbations in tokamaks', Submitted to Plasma Phys. Control. Fusion
- [9] Y. Song *et al.*, 2014 IEEE Trans. Plasma Sci. **42**, 415
- [10] M. Jia *et al.*, 2014, submitted to PPCF
- [11] G. Li *et al.*, 2013 Plasma Phys. Control. Fusion **55**, 125008